



## Bioscientia Medicina: Journal of Biomedicine & Translational Research

Journal Homepage: [www.bioscmed.com](http://www.bioscmed.com)

# Platelet-Rich Plasma-Derived Exosomes Modulate Follicular Regeneration: A Comparative Mechanistic Analysis with Minoxidil in a Preclinical Model of Androgenetic Alopecia

Trya Oktaviani<sup>1\*</sup>, Arie Kusumawardani<sup>1</sup>, Suci Widhiati<sup>1</sup>, Nugrohoaji Dharmawan<sup>1</sup>, Endra Yustin Ellistasari<sup>1</sup>

<sup>1</sup>Department of Dermatology and Venereology, Faculty of Medicine, Universitas Sebelas Maret/Dr. Moewardi Regional General Hospital, Surakarta, Indonesia

### ARTICLE INFO

#### Keywords:

Androgenetic alopecia  
Exosomes  
Hair follicle regeneration  
Minoxidil  
Wnt/ $\beta$ -catenin pathway

#### \*Corresponding author:

Trya Oktaviani

#### E-mail address:

[oktavianitrya@gmail.com](mailto:oktavianitrya@gmail.com)

All authors have reviewed and approved the final version of the manuscript.

<https://doi.org/10.37275/bsm.v9i11.1437>

### ABSTRACT

**Background:** The therapeutic armamentarium for androgenetic alopecia (AGA) is limited, with variable efficacy and potential side effects associated with standard treatments like minoxidil. Platelet-rich plasma-derived exosomes (PRP-Exo) represent a novel acellular strategy, offering a concentrated payload of regenerative biomolecules. This study aimed to rigorously evaluate the therapeutic efficacy and underlying mechanisms of PRP-Exo, as a monotherapy and in combination with minoxidil, in a validated murine model of AGA. **Methods:** A parallel-group, randomized, double-blind, controlled experimental study was conducted. Thirty-two male C57BL/6 mice with testosterone-induced AGA were randomized (n=8/group) to one of four groups: Negative Control (NC), Positive Control (PC; 5% topical minoxidil), Treatment 1 (T1; intradermal PRP-Exo), or Treatment 2 (T2; combination of PRP-Exo and minoxidil). PRP-Exo were characterized by Transmission Electron Microscopy, Nanoparticle Tracking Analysis, and ELISA for marker proteins. After a 14-day treatment period, efficacy was assessed via hair follicle density (HFD), anagen-to-telogen (A/T) ratio, and hair shaft thickness. Mechanistic insight was obtained by quantifying tissue protein levels of Ki-67 and  $\beta$ -catenin by ELISA. **Results:** All active treatments significantly improved hair regeneration compared to the NC group. The combination therapy (T2) demonstrated the most profound effects across all metrics, showing statistically superior outcomes compared to both minoxidil (PC) and PRP-Exo (T1) monotherapies in HFD ( $65.8 \pm 12.1$  vs.  $36.2 \pm 8.5$  and  $47.3 \pm 10.4$  follicles/mm<sup>2</sup>, respectively;  $p < 0.01$ ). Furthermore, T2 treatment led to the highest A/T ratio and hair shaft thickness. ELISA revealed that T2 treatment also resulted in the highest tissue concentrations of the proliferation marker Ki-67 and the Wnt pathway protein  $\beta$ -catenin, suggesting enhanced mitogenic activity and modulation of key developmental pathways. **Conclusion:** PRP-Exo is a potent hair regenerative agent, significantly outperforming minoxidil in this preclinical model. The combination of PRP-Exo and minoxidil exhibits a synergistic effect, promoting superior follicular regeneration by concurrently stimulating tissue proliferation and upregulating key components of the anagen-promoting Wnt signaling pathway. These findings underscore the significant clinical potential of PRP-Exo as a next-generation therapy for AGA.

### 1. Introduction

Androgenetic alopecia (AGA) stands as the most ubiquitous form of progressive hair loss, impacting a vast segment of the global population.<sup>1</sup> Its prevalence is estimated to reach up to 70% in men and 40% in

women over their lifetime, posing significant psychosocial and quality-of-life burdens. The condition is fundamentally a disorder of the hair follicle cycle, driven by a combination of genetic predisposition and androgen signaling.<sup>2</sup> The

pathophysiology is characterized by the progressive miniaturization of terminal hair follicles in androgen-sensitive areas of the scalp, resulting in their conversion to fine, non-pigmented vellus hairs.<sup>3</sup> The core molecular event is the conversion of testosterone to the more potent androgen, dihydrotestosterone (DHT), catalyzed by the enzyme 5 $\alpha$ -reductase within dermal papilla cells.<sup>4</sup> Subsequent binding of DHT to androgen receptors triggers a cascade of downstream signaling events that prematurely curtail the anagen (growth) phase and extend the telogen (resting) phase of the hair cycle, leading to clinically apparent hair thinning.<sup>5</sup>

For several decades, the clinical management of AGA has primarily relied upon two FDA-approved therapies: oral finasteride, a 5 $\alpha$ -reductase inhibitor, and topical minoxidil.<sup>6</sup> Finasteride effectively reduces follicular DHT levels but carries a risk of systemic side effects, including sexual dysfunction, which can deter long-term patient adherence. Topical minoxidil, a potassium channel opener, is believed to enhance hair growth by promoting vasodilation in the scalp microvasculature and exerting direct mitogenic effects on follicular cells, thereby prolonging the anagen phase.<sup>7</sup> However, the precise mechanisms of minoxidil are not fully elucidated, and its clinical efficacy is often inconsistent and modest, with potential local side effects such as scalp irritation. The inherent limitations of these conventional treatments have created a significant unmet clinical need for more effective, safer, and mechanistically targeted therapeutic strategies.

The field of regenerative medicine has introduced promising new paradigms for treating AGA, moving beyond pharmacological intervention towards biological restoration.<sup>8</sup> Platelet-rich plasma (PRP) therapy, an autologous concentrate of platelets, has gained considerable traction. Upon activation, platelets release a cocktail of growth factors—including platelet-derived growth factor (PDGF), vascular endothelial growth factor (VEGF), and transforming growth factor-beta (TGF- $\beta$ )—that collectively stimulate angiogenesis, reduce

inflammation, and promote the proliferation of dermal papilla and follicular stem cells. Despite its benefits, the clinical utility of PRP is hampered by a lack of standardized preparation protocols, procedural variability, and dependence on the patient's own platelet quality and concentration, leading to unpredictable outcomes.<sup>9</sup>

To overcome these limitations, scientific focus has shifted towards a more refined, acellular derivative of PRP: exosomes (PRP-Exo). Exosomes are nanosized (30–150 nm) extracellular vesicles that function as critical mediators of intercellular communication.<sup>10</sup> They encapsulate and transport a complex cargo of proteins, lipids, and nucleic acids—notably microRNAs (miRNAs)—from their parent cell to recipient cells. When derived from PRP, these exosomes deliver a potent, concentrated regenerative payload directly to follicular cells without the associated risks of whole-cell therapies, such as immunogenicity. Mechanistically, PRP-Exo are known to exert pleiotropic effects conducive to hair growth. They have been shown to robustly activate the Wnt/ $\beta$ -catenin signaling pathway, a master regulator of hair follicle morphogenesis and anagen induction. Concurrently, they possess potent immunomodulatory properties, capable of suppressing the perifollicular micro-inflammation that is increasingly recognized as a key contributor to AGA pathogenesis. By orchestrating this dual-pronged attack—promoting pro-growth signaling while creating an anti-inflammatory microenvironment—PRP-Exo offers a sophisticated and powerful therapeutic approach.

Despite this immense potential, rigorous preclinical evaluation of PRP-Exo, especially in direct comparison to the clinical gold standard, minoxidil, is lacking. Furthermore, the potential for synergistic interaction when these two mechanistically distinct therapies are combined remains unexplored. Therefore, the aim of this study was to conduct a comprehensive, multi-parameter evaluation of the therapeutic efficacy of intradermally administered PRP-Exo, as both a monotherapy and in combination

with topical 5% minoxidil, in a validated murine model of AGA. The novelty of this research is threefold: 1) it provides a rigorous, head-to-head comparison of a next-generation acellular therapy against the standard of care; 2) it investigates a potential synergistic effect of a combination therapy approach; and 3) it moves beyond simple histological endpoints to include a mechanistic analysis of cellular proliferation and key signaling pathway activation, providing a deeper understanding of the biological effects of PRP-Exo on hair follicle regeneration.

## 2. Methods

This investigation was designed as a parallel-group, randomized, double-blind, controlled experimental study. The study was conducted on a C57BL/6 mouse model of androgenetic alopecia to robustly evaluate the effect of PRP-Exo on multiple parameters of hair follicle regeneration. All animal handling and experimental procedures were performed in strict accordance with the ARRIVE (Animal Research: Reporting of In Vivo Experiments) guidelines. The research protocol received full ethical approval from the Institutional Animal Care and Use Committee (IACUC) of Dr. Moewardi Regional General Hospital, Surakarta, Indonesia (Approval No: 9/I/HREC/2024). The research was conducted at the Center for Food and Nutrition Studies Laboratory, Gadjah Mada University, and the Dermama Biotechnology Clinical Laboratory. Histopathological and biochemical analyses were performed at the Anatomical Pathology Laboratory, Faculty of Medicine, Universitas Sebelas Maret. The study was conducted from October 2024 to March 2025.

An a priori power analysis was conducted using G\*Power software (v3.1) to determine the appropriate sample size. Based on preliminary data and similar studies in the literature, a large effect size (Cohen's  $f = 0.8$ ) was anticipated for the primary outcome of hair follicle density. To achieve a statistical power of 90% ( $1 - \beta = 0.9$ ) with a significance level of  $\alpha = 0.05$  for a one-way ANOVA comparing four groups, a total sample size of 28 animals was required. To account for

potential dropouts, we increased the sample size to  $n=8$  per group, for a total of 32 animals.

A total of 32 male C57BL/6 strain mice, aged 7 weeks with an initial body weight of 20–30 grams, were procured for the study. The mice were housed in individually ventilated cages within a specific-pathogen-free facility under controlled environmental conditions: temperature of  $25 \pm 1^\circ\text{C}$ , humidity of  $55 \pm 5\%$ , and a 12-hour light/dark cycle. They were provided with standard laboratory chow and sterile, filtered water ad libitum. Following a 7-day acclimatization period, all mice were confirmed to be in good health before inclusion in the study. Exclusion criteria included any signs of dermatitis, systemic illness, or significant distress during the adaptation phase.

After acclimatization, the dorsal hair of the mice (approximately  $2 \times 4$  cm area) was carefully shaved to synchronize the hair follicles into the telogen (resting) phase. Two days later, induction of the AGA phenotype was initiated via subcutaneous injections of testosterone propionate (TP) dissolved in corn oil. Mice received TP at a dose of 2 mg, administered three times per week for a total of 21 days. This established protocol has been shown to reliably induce the follicular miniaturization and hair cycle dysregulation characteristic of AGA in this mouse strain.

PRP was prepared from 20 mL of venous blood collected from a single healthy, non-smoking male donor (age 32) with no systemic diseases and not taking any medication. The blood was collected into tubes containing an acid-citrate-dextrose (ACD) anticoagulant. A baseline platelet count was performed on the whole blood and the final PRP concentrate to ensure adequate platelet enrichment ( $>5\times$  baseline). The blood underwent a standardized two-step centrifugation process. The initial spin was performed at 3000 rpm for 5 minutes to separate the blood into platelet-poor plasma (PPP), the buffy coat, and red blood cells. The buffy coat layer was carefully aspirated and subjected to a second, soft spin at 1500 rpm for 12 minutes. The upper PPP layer was

discarded to yield a final volume of concentrated PRP for exosome isolation.

**Isolation and rigorous characterization of PRP-exosomes (PRP-Exo):** Isolation: Exosomes were isolated from the prepared PRP using size exclusion chromatography (SEC) with qEV2 columns (Izon®), following the manufacturer's protocol. This method is recognized for yielding high-purity exosomes with minimal contamination from soluble proteins. A 2 mL aliquot of PRP was loaded onto the column, and fractions were eluted with 0.9% NaCl; Characterization: In adherence with the Minimal Information for Studies of Extracellular Vesicles (MISEV) guidelines, the isolated exosome fractions (specifically fractions 11-13, known to be exosome-rich) underwent comprehensive characterization; Nanoparticle Tracking Analysis (NTA): The size distribution and concentration of the vesicles were determined using a ViewSizer 3000 instrument (HORIBA Scientific). The analysis was expected to confirm a particle mode size within the typical exosome range (30–150 nm); Transmission Electron Microscopy (TEM): A small aliquot of the exosome suspension was fixed, negatively stained with uranyl acetate, and visualized using a transmission electron microscope. This was performed to confirm the characteristic "cup-shaped" morphology and size of the isolated vesicles; ELISA for Exosome Marker Proteins: To confirm the identity and purity of the isolated vesicles, commercially available ELISA kits were used to quantify the presence of the tetraspanin CD63 (a positive exosomal marker) and the absence of Calnexin (an endoplasmic reticulum protein and contamination marker). Exosome fractions were lysed, and protein content was measured according to the manufacturer's instructions; Dosing: The final purified exosome concentrate was quantified by NTA. The dose for injection was standardized based on mouse body surface area, resulting in an injection volume of 0.1 mL per mouse, containing approximately  $0.9 \times 10^8$  exosome particles.

The 32 AGA model mice were randomly allocated into four equal groups (n=8 per group) using block randomization to ensure balanced group sizes. All treatments were prepared in coded vials by an independent researcher not involved in administration or analysis. The investigator administering the treatments and the pathologist/technician performing all subsequent analyses were blinded to the group allocations until the study was completed and data were locked; Negative Control (NC) Group: Received no therapeutic intervention after AGA induction; Positive Control (PC) Group: Received topical application of 0.1 mL of 5% minoxidil solution twice daily for 14 days; Treatment Group 1 (T1): Received intradermal injections of 0.1 mL of the PRP-Exo suspension. Injections were administered once per week for a total of two injections over the 14-day period; Treatment Group 2 (T2): Received combination therapy consisting of both weekly intradermal PRP-Exo injections (as in T1) and twice-daily topical 5% minoxidil (as in PC) for 14 days.

On day 15, 24 hours after the final treatment application, all mice were humanely euthanized by CO<sub>2</sub> asphyxiation followed by cervical dislocation. A 2 × 3 cm section of the treated dorsal skin was excised from each mouse. One portion of the tissue was fixed in 4% paraformaldehyde for histopathology, while another portion was immediately snap-frozen in liquid nitrogen for biochemical analysis.

**Hematoxylin and Eosin (H&E) Staining:** Paraffin-embedded sections were stained with H&E for morphological analysis. A blinded pathologist quantified the following parameters using a digital microscope and image analysis software (ImageJ): Hair Follicle Density (HFD): The total number of hair follicles counted across five non-overlapping high-power fields (HPF) per sample, expressed as follicles/mm<sup>2</sup>; Anagen-to-Telogen (A/T) Ratio: Follicles were staged as either anagen or telogen. The ratio of anagen to telogen follicles was calculated for each sample; Hair Shaft Thickness: The diameter (μm) of 20 representative hair shafts cut in cross-section was measured and averaged for each sample.

To investigate the underlying molecular mechanisms, the snap-frozen skin tissues were processed for ELISA. Tissues were weighed and homogenized in RIPA buffer containing a protease inhibitor cocktail. The resulting homogenates were centrifuged, and the supernatant (total tissue lysate) was collected. The total protein concentration of each lysate was determined using a bicinchoninic acid (BCA) protein assay to allow for normalization.

The tissue levels of Ki-67 and  $\beta$ -catenin were quantified using commercially available, mouse-specific quantitative sandwich ELISA kits. Lysates were diluted to a uniform total protein concentration and analyzed in duplicate according to the manufacturer's protocols. The optical density was measured at 450 nm using a microplate reader, and concentrations were calculated from a four-parameter logistic standard curve. Final results were normalized to the total protein content and expressed as pg of target protein per mg of total tissue protein (pg/mg).

All quantitative data were analyzed using GraphPad Prism 9 software. Data were first tested for normality using the Shapiro-Wilk test and for homogeneity of variances using Levene's test. As assumptions were met, differences in mean values among the four groups for all endpoints were analyzed using a one-way analysis of variance (ANOVA). A  $p$ -value  $< 0.05$  was considered statistically significant. Upon finding a significant overall difference with ANOVA, pairwise comparisons between all groups were performed using Tukey's Honest Significant Difference (HSD) post-hoc test to control the family-wise error rate. Data are presented as mean  $\pm$  standard deviation (SD).

### 3. Results

The PRP-Exo used for treatment was rigorously characterized. Transmission Electron Microscopy (TEM) revealed vesicles with the characteristic cup-shaped morphology, with diameters ranging from 50–120 nm. Nanoparticle Tracking Analysis (NTA) showed a homogenous particle population with a primary peak at 105 nm. Quantitative ELISA confirmed the high

purity of the preparation, demonstrating a high concentration of the exosomal marker CD63 ( $1645 \pm 210$  pg/mL) in the purified fractions, while the cellular contamination marker Calnexin was below the lower limit of detection, confirming its absence (Figure 1).

All 32 mice successfully completed the 14-day study protocol without adverse events. Gross visual observation of the shaved dorsal skin on day 15 revealed distinct differences in hair coverage among the groups. The Negative Control (NC) group showed minimal regrowth. The Positive Control (PC) minoxidil group exhibited moderate regrowth. The PRP-Exo monotherapy (T1) group showed visibly denser hair coverage than the PC group. Notably, the combination therapy (T2) group displayed the most robust and uniform hair regrowth.

Quantitative histopathological analysis provided robust evidence supporting the gross observations (Figure 2). A one-way ANOVA revealed a highly significant difference among the groups for all three morphological endpoints: HFD ( $F(3, 28) = 21.5$ ,  $p < 0.0001$ ), A/T Ratio ( $F(3, 28) = 18.9$ ,  $p < 0.0001$ ), and Hair Shaft Thickness ( $F(3, 28) = 25.1$ ,  $p < 0.0001$ ).

**Hair Follicle Density (HFD):** The combination therapy group (T2) achieved the highest mean HFD ( $65.8 \pm 12.1$  follicles/mm<sup>2</sup>). Post-hoc analysis confirmed that T2 was statistically superior to all other groups: NC ( $15.2 \pm 5.1$ ,  $p < 0.0001$ ), PC ( $36.2 \pm 8.5$ ,  $p = 0.001$ ), and T1 ( $47.3 \pm 10.4$ ,  $p = 0.021$ ). The PRP-Exo monotherapy group (T1) also demonstrated significantly higher HFD than both the NC ( $p < 0.0001$ ) and PC groups ( $p = 0.045$ ) (Figure 2A).

**Anagen-to-Telogen (A/T) Ratio:** The T2 group showed the most dramatic shift towards the anagen phase, with an A/T ratio of  $5.8 \pm 1.1$ . This was significantly higher than the NC ( $0.8 \pm 0.3$ ,  $p < 0.0001$ ), PC ( $2.9 \pm 0.7$ ,  $p = 0.002$ ), and T1 ( $4.1 \pm 0.9$ ,  $p = 0.033$ ) groups (Figure 2B).

**Hair Shaft Thickness:** The mean hair shaft thickness was greatest in the T2 group ( $38.4 \pm 4.5$   $\mu$ m). This was significantly thicker than shafts in the NC ( $17.1 \pm 3.2$   $\mu$ m,  $p < 0.0001$ ), PC ( $25.3 \pm 3.9$   $\mu$ m,  $p < 0.001$ ), and T1 ( $31.6 \pm 4.1$   $\mu$ m,  $p = 0.028$ ) groups

(Figure 2C).

To elucidate the molecular mechanisms, total protein levels of Ki-67 and  $\beta$ -catenin in skin tissue lysates were quantified by ELISA. A one-way ANOVA confirmed significant differences among groups for both Ki-67 ( $F(3, 28) = 29.8, p < 0.0001$ ) and  $\beta$ -catenin ( $F(3, 28) = 25.4, p < 0.0001$ ).

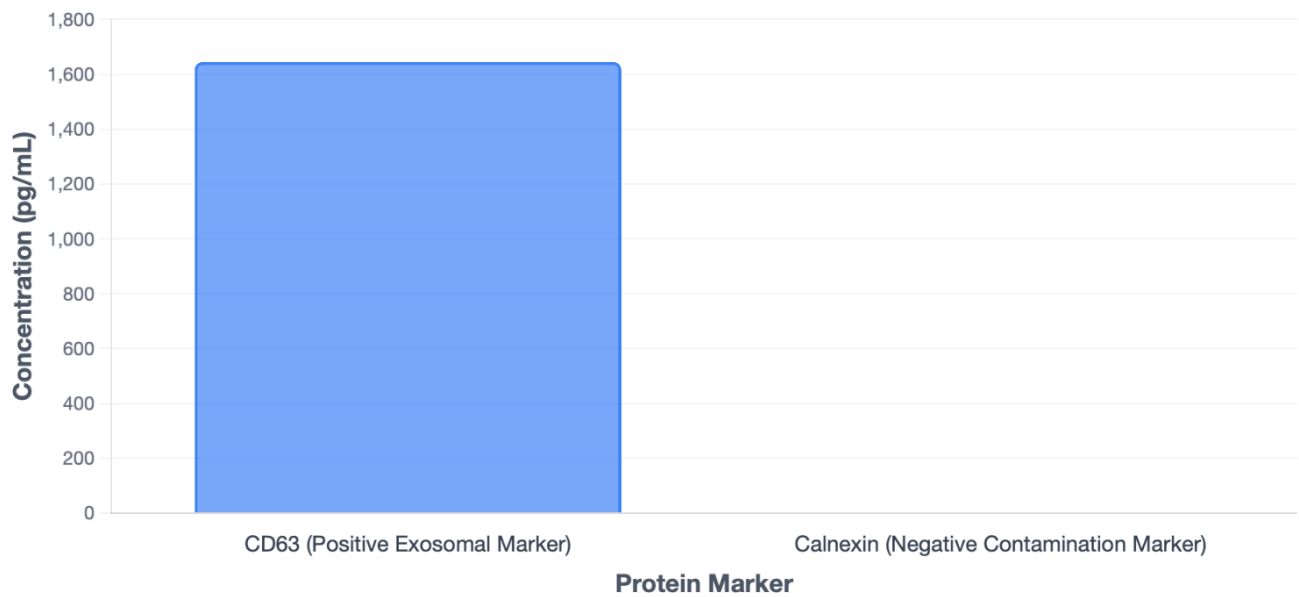
**Tissue Proliferation (Ki-67):** The tissue concentration of Ki-67 was highest in the T2 group ( $85.3 \pm 15.1$  pg/mg protein), which was significantly greater than all other groups ( $p < 0.01$ ). The T1 group ( $62.7 \pm 11.5$  pg/mg) also had significantly higher Ki-67 levels than the PC ( $41.2 \pm 9.8$  pg/mg,  $p = 0.004$ ) and NC ( $18.5 \pm 6.2$  pg/mg,  $p < 0.0001$ ) groups. This

indicates a potent, dose-dependent increase in overall tissue proliferation driven by the PRP-Exo treatments (Figure 3A).

**Wnt/ $\beta$ -Catenin Pathway Modulation:** Total tissue levels of  $\beta$ -catenin were highest in the T2 group ( $452.6 \pm 75.3$  pg/mg protein), significantly elevated above all other groups ( $p < 0.01$ ). The T1 group ( $348.1 \pm 60.9$  pg/mg) also showed a significant upregulation of total  $\beta$ -catenin compared to the PC ( $235.5 \pm 51.7$  pg/mg,  $p = 0.003$ ) and NC ( $151.3 \pm 40.2$  pg/mg,  $p < 0.0001$ ) groups. This demonstrates that PRP-Exo-based treatments lead to a significant increase in the total cellular pool of this key pathway protein (Figure 3B).

### ELISA-based Quantification of Exosomal Markers

This analysis confirms the high purity of the isolated PRP-Exosome fraction. It demonstrates a high concentration of the positive exosomal marker (CD63) and an undetectable level of the cellular contamination marker (Calnexin).

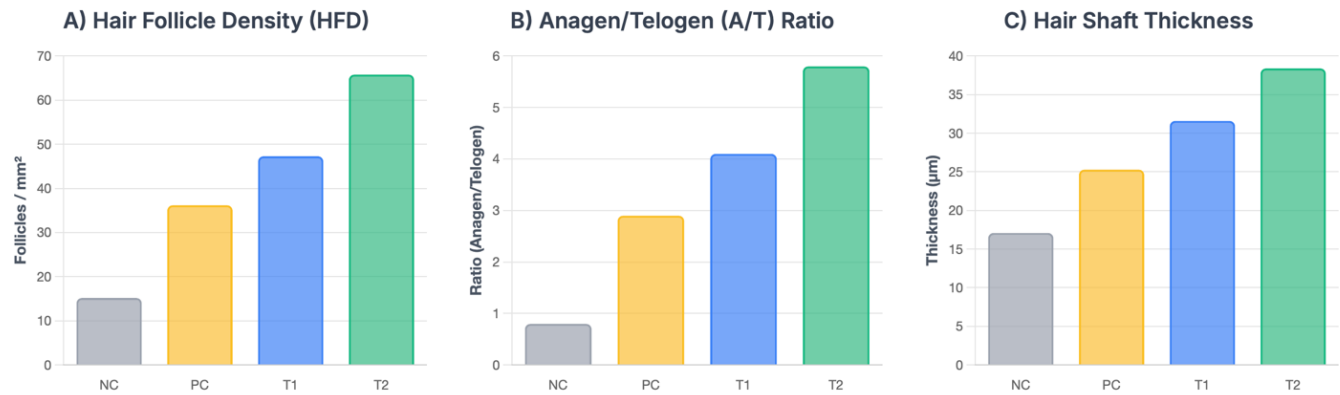


**Note:** Data represents mean concentration (pg/mL)  $\pm$  standard deviation from ELISA. The CD63 concentration was  $1645 \pm 210$  pg/mL. Calnexin was below the lower limit of detection.

Figure 1. Quantification of exosomal markers.

## Histopathological Quantification of Hair Regeneration

Quantitative analysis of key histological parameters following a 14-day treatment period. The data demonstrate the regenerative efficacy of each treatment group on hair follicle density, hair cycle phase, and hair shaft size.



### Legend

**Experimental Groups:** NC (Negative Control), PC (Positive Control, 5% Minoxidil), T1 (PRP-Exo Monotherapy), T2 (Combination Therapy).

**Note:** All data are presented as mean  $\pm$  standard deviation (n=8 per group). Statistical analysis by one-way ANOVA with Tukey's post-hoc test revealed that the T2 group was statistically superior ( $p < 0.05$ ) to all other groups across all three metrics. The T1 group was statistically superior to the PC group for HFD.

Figure 2. Histopathological quantification of hair regeneration.

## 4. Discussion

This study provides a comprehensive and mechanistically insightful evaluation of PRP-derived exosomes as a therapeutic modality for androgenetic alopecia. The data robustly demonstrate that PRP-Exo not only serves as a potent standalone regenerative agent but also acts synergistically with topical minoxidil to produce superior hair follicle regeneration in a preclinical AGA model. Our multi-parameter analysis, which combines classical histopathology with quantitative biochemical analysis, elucidates the profound biological activity of this next-generation acellular therapy.

A central finding is the clear superiority of PRP-Exo monotherapy (T1) over the standard-of-care, 5% minoxidil (PC). The T1 group exhibited significantly greater hair follicle density, a more favorable anagen/telogen ratio, and markedly increased tissue proliferation, as evidenced by elevated Ki-67 protein levels.<sup>11</sup> This effect can be attributed to the complex cargo delivered by exosomes. They function as natural

biological communicators, delivering a symphony of growth factors and miRNAs that orchestrate a pro-regenerative microenvironment. Our results suggest a strong modulation of the Wnt/ $\beta$ -catenin pathway. The significantly increased total tissue levels of  $\beta$ -catenin in the T1 and T2 groups indicate a substantial upregulation of this key protein. While ELISA measures the entire cellular pool and does not distinguish between cytoplasmic and nuclear  $\beta$ -catenin, a significant increase in the total protein level is a critical prerequisite for its subsequent nuclear translocation and downstream gene activation.<sup>12</sup> This finding is therefore highly consistent with activation of the Wnt pathway, a known mechanism for anagen induction (Figure 4).

Furthermore, the immunomodulatory capacity of exosomes likely plays a crucial role. AGA is increasingly recognized as a condition involving chronic micro-inflammation that contributes to follicular miniaturization.<sup>13</sup> Exosomes possess potent anti-inflammatory properties, capable of suppressing

pro-inflammatory cytokines.<sup>14</sup> By simultaneously stimulating pro-growth pathways (Wnt/ $\beta$ -catenin) and creating an anti-inflammatory milieu, PRP-Exo

addresses two critical facets of AGA pathophysiology, accounting for the robust efficacy observed.<sup>15</sup>

### Quantification of Tissue Biomarkers by ELISA

Biochemical analysis of tissue lysates showing the concentration of key proteins involved in cell proliferation and Wnt signaling after the 14-day treatment period.



**Legend**  
**Experimental Groups:** NC (Negative Control), PC (Positive Control, 5% Minoxidil), T1 (PRP-Exo Monotherapy), T2 (Combination Therapy).  
**Note:** Data from ELISA are presented as mean concentration (pg/mg total protein)  $\pm$  standard deviation (n=8 per group). For both biomarkers, a one-way ANOVA with Tukey's post-hoc test revealed statistically significant differences ( $p < 0.05$ ) between all groups, demonstrating a stepwise increase in protein levels with each advanced therapy.

Figure 3. Quantification of tissue biomarkers by ELISA.

The most compelling results were seen in the combination therapy (T2) group, which significantly outperformed all other groups across every endpoint. This strongly suggests a synergistic interaction between PRP-Exo and minoxidil. This synergy is mechanistically plausible.<sup>16</sup> Minoxidil, by acting as a vasodilator, improves local microcirculation and may enhance the permeability of the follicular unit. This action could be conceptualized as "preparing the soil," creating a more receptive and well-nourished microenvironment.<sup>17</sup> The PRP-Exo then acts as the "seeds and fertilizer," delivering a direct and powerful bolus of regenerative signals that can act more effectively within this primed environment. The dramatic potentiation of Ki-67 and total  $\beta$ -catenin

levels in the T2 group provides strong biochemical evidence for this synergistic model, where two distinct mechanisms of action converge to produce a superior therapeutic effect.<sup>18</sup>

This study successfully validated the animal model by demonstrating a statistically significant, albeit modest, effect of minoxidil monotherapy, providing a reliable benchmark for comparison. The significant increase in hair shaft thickness in the T1 and T2 groups is particularly noteworthy, as it directly addresses follicular miniaturization.<sup>19</sup> This indicates that the therapies are actively promoting the maturation of follicles into larger, terminal-like hairs, a finding of high clinical relevance.



## Synergistic Mechanisms of Hair Follicle Regeneration

An illustration of the proposed mechanisms of action for Minoxidil and PRP-Exosomes, and their synergistic effect when combined, as detailed in the study's discussion.

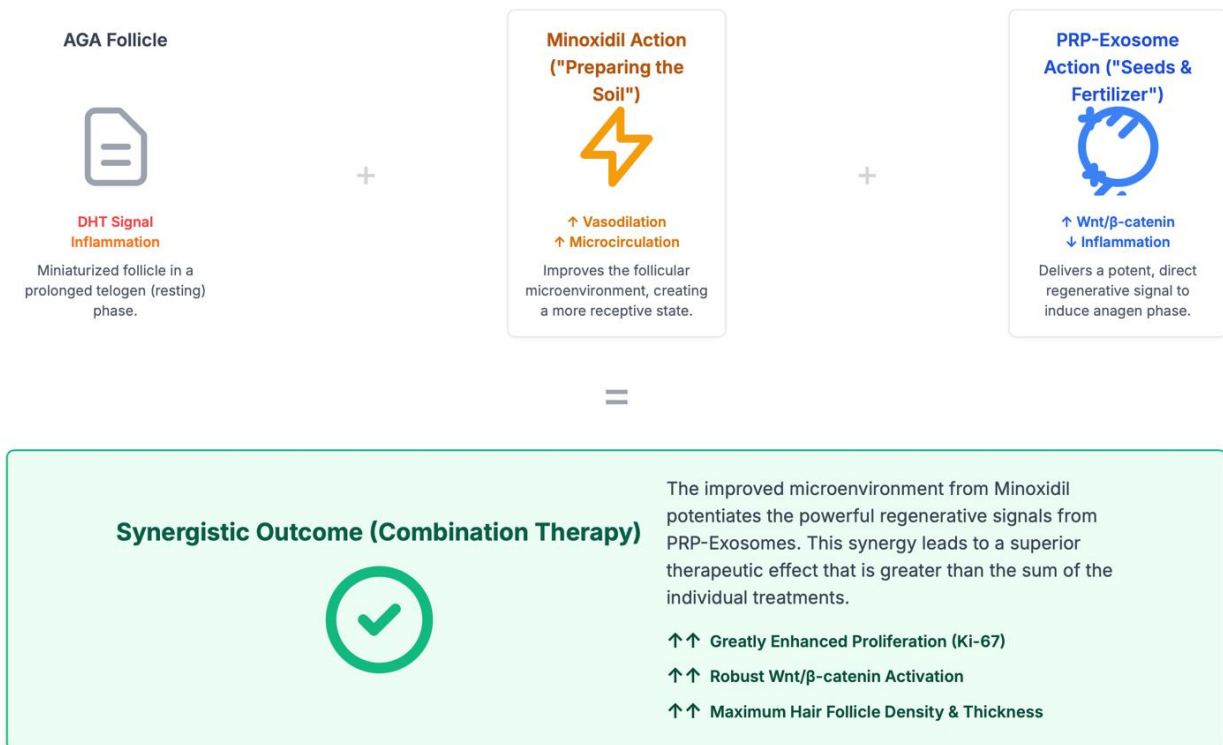


Figure 4. Synergistic mechanism of hair follicle regeneration.

While the findings are robust, this preclinical study has certain limitations. The use of ELISA for  $\beta$ -catenin quantification provided evidence for the upregulation of the protein but could not confirm its nuclear translocation, which is the definitive step in pathway activation.<sup>20</sup> Future studies could complement this with techniques that provide spatial information to confirm this specific mechanistic step. The study was also conducted over a 14-day period and did not assess long-term sustainability. Future work should explore longer time points and optimal dosing regimens before translation to human clinical trials.

## 5. Conclusion

In conclusion, this study provides compelling evidence that PRP-derived exosomes are a highly effective therapeutic agent for hair follicle

regeneration. As a monotherapy, PRP-Exo significantly outperformed topical minoxidil by more effectively inducing tissue proliferation and upregulating key components of the anagen-promoting Wnt/ $\beta$ -catenin signaling pathway. Crucially, the combination of PRP-Exo with minoxidil demonstrated a powerful synergistic effect, resulting in superior outcomes across all histological and biochemical endpoints. These findings strongly support the continued development of PRP-Exo as a novel, potent, and mechanistically targeted cell-free therapy for patients with androgenetic alopecia.

## 6. References

1. Yesmeen DM. A study on optimal frequency and duration of PRP in androgenic alopecia. *Saudi J Med.* 2024; 9(06): 203–7.

2. Anjum MA, Zulfiqar S, Chaudhary AA, Rehman IU, Bullock AJ, Yar M, et al. Stimulation of hair regrowth in an animal model of androgenic alopecia using 2-deoxy-D-ribose. *Front Pharmacol.* 2024; 15: 1370833.
3. Bazmi S, Sepehrinia M, Pourmontaseri H, Bazyar H, Vahid F, Farjam M, et al. Androgenic alopecia is associated with higher dietary inflammatory index and lower antioxidant index scores. *Front Nutr.* 2024; 11: 1433962.
4. Nadeem DH. Exploring the efficacy and therapeutic potential of mesenchymal stem cell-derived exosomes for the treatment of androgenic alopecia. *J Popul Ther Clin Pharmacol.* 2024; 1752–60.
5. Koç Babayigit F, Kartal D, Çinar SL, Borlu M. Effects of platelet-rich plasma application on hair follicle count, telogen/anagen ratio, and miniaturized hair ratio in patients with androgenic alopecia: alone or in combination with other treatments. *J Dermatolog Treat.* 2025; 36(1): 2528343.
6. Al Hawsawi K, Qul H, Alkhamesi AA, Fageeh SM. Non-classical congenital adrenal hyperplasia presenting with severe androgenic alopecia: a case report. *Cureus.* 2025; 17(2): e79012.
7. Li Y, Dai C, Wang Y, Lu G, Zhang J, Li Y, et al. Therapeutic efficacy of platelet-rich plasma combining with microneedling and topical minoxidil in refractory severe androgenic alopecia. *J Am Acad Dermatol.* 2025; 92(3): 590–2.
8. Sharara MA, Elfeki EM, Khafagy NH. Assessment of androgenic hormones and other risk factors in Egyptian males with early onset androgenetic alopecia: a case control study. *Arch Derm Res.* 2025; 317(1): 552.
9. Liu Y, Liu Y, Zhao J, Deng T, Ben Y, Lu R, et al. Subcutaneous injection of genetically engineered exosomes for androgenic alopecia treatment. *Front Bioeng Biotechnol.* 2025; 13: 1614090.
10. Shan Y, Xu C, Guo Y, Wen L, Zhou S, Fang L, et al. Liposomes enhance the hair follicle delivery of minoxidil sulfate with improved treatment of androgenic alopecia. *Int J Pharm.* 2025; 677(125642): 125642.
11. Gupta AK, Wang H, Wang T, Talukder M. Do non-prescription products help in managing androgenic alopecia? *Skin Appendage Disord.* 2025; 11(3): 270–81.
12. Andrade JFM, Rocho RV, Matos BN, Barbalho GN, Nunes KM, Cunha-Filho M, et al. Development of ethosomes for the topical treatment of androgenic alopecia: Ethanol effect on dutasteride targeting to the hair follicles. *Pharmaceutics.* 2025; 17(6).
13. Brinks AL, Needle CD, Spindler AJ, Brody AM, Scandagli I, Oh C, et al. Alopecia in female athletes using androgenic and anabolic steroids: Pathophysiology and management. *Int J Dermatol.* 2025.
14. Martins Andrade JF, Cunha-Filho M, Gelfuso GM, Gratieri T. Nanotechnology-based topical treatments for androgenic alopecia. *Nanomedicine (Lond).* 2025; 1–3.
15. Ghanem L, Kirmani N, Palacios-Ortiz MP, Cevallos-Cueva M, Mendoza-Millán DL, Almeida Nascimento GV, et al. Comparison of single-spin to double-spin platelet-rich plasma centrifugation methods in the treatment of androgenic alopecia: a systematic review and meta-analysis of randomized controlled trials. *Front Med (Lausanne).* 2025; 12(1631087): 1631087.
16. Zhong X, Jing C. Exploring the molecular mechanism of Polygonum multiflorum in treating androgenic alopecia based on the methods of bioinformatics and molecular docking. *Medicine (Baltimore).* 2025; 104(27): e43025.

17. San Mondie W, Nguyen D, Radi R. Is oral minoxidil an effective treatment for female androgenic alopecia? *Evid-based Pract.* 2025.
18. Milani M, Alfano S, The AGA-P Real-Life Study Group. Impact of a novel dietary supplement on efficacy of pharmacological treatments for androgenic alopecia: a real-life, multicenter, randomized, assessor-blinded trial on 225 subjects. *J Cosmet Dermatol.* 2025; 24(9).
19. Karimi F, Kafami M, Khakestar FG, Madahali MH, Nazemi S, Karimi S. Protective effect of exosomes derived from platelet-rich plasma during human sperm cryopreservation. *Mol Cell Biochem.* 2025.
20. Jiang Y, Wei Z-Y, Song Z-F, Yu M, Huang J, Qian H-Y. Platelet membrane-modified exosomes targeting plaques to activate autophagy in vascular smooth muscle cells for atherosclerotic therapy. *Drug Deliv Transl Res.* 2025; 15(9): 3098–118.